Vortex Avalanches in the Non-centrosymmetric Superconductor Li_2Pt_3B

C. F. Miclea[1], M. B. Maple[2], C. McElroy[2], A. C. Mota[1,3], T. A. Sayles[2], M. Sigrist[4], B. J. Taylor[2], and F. Steglich[1]

We investigated the vortex dynamics in the non-centrosymmetric superconductor Li_2Pt_3B in the $0.1\ K \leq T \leq 2.8\ K$ temperature range. Two different logarithmic creep regimes in the decay of the remanent magnetization from the Bean critical state have been observed. In the first regime, the creep rate is extraordinarily small, indicating the existence of a new, very effective pinning mechanism. At a certain time, a vortex avalanche occurs that increases the logarithmic creep rate by a factor of about 5 to 10, depending on the temperature. This may indicate that certain barriers against flux motion are present and can be opened under increased pressure exerted by the vortices.

The occurrence of superconductivity in compounds with non-centrosymmetric crystal structures has recently attracted considerable attention. Besides various other systems, superconductivity has also been reported in the ternary boride compounds Li_2Pd_3B and Li_2Pt_3B which have superconducting critical temperatures of 7-8 K and 2.4 K, respectively [1,2]. These two isostructural compounds crystallize in a structure consisting of distorted boron centered octahedra of BPd_6 or BPt_6 in an approximately cubic arrangement with an inter-penetrating lithium formation [3]. Both substructures, hence the composite crystal structure, lack inversion symmetry. Several unusual properties appear in non-centrosymmetric superconductors depending on various factors, particularly the specific form of the spin-orbit coupling in such systems as well as the pairing symmetry [4-6]. In contrast to the strongly correlated non-centrosymmetric heavy fermion superconductors $CePt_3Si$ [7], $CeRhSi_3$ [8], and UIr [9] for which superconductivity is associated with a magnetic quantum phase transition, there is no evidence of magnetic order or strong electronic correlations in either Li_2Pd_3B or Li_2Pt_3B. Measurements of the London penetration depth suggest that Li_2Pd_3B has a full quasiparticle gap in the superconducting phase, while for Li_2Pt_3B, the data indicate line nodes in the energy gap [10]. NMR measurements [11] suggest that Li_2Pd_3B is a spin singlet, s-wave superconductor. By contrast, in Li_2Pt_3B, the spin susceptibility measured by the Knight shift remains unchanged across the superconducting transition temperature. Moreover, the spin-lattice relaxation rate $1/T_1$ shows no coherence peak below T_c, decreasing as T^3 with decreasing temperature, consistent with line nodes in the superconducting gap. Here, we investigate a further intriguing property of the unconventional superconductor Li_2Pt_3B, observed in the vortex dynamics. We demonstrate that the behavior of the flux creep is very unusual, displaying at short times extremely small creep rates, followed by a faster avalanche-like escape of magnetic flux.

Samples of Li_2Pt_3B used in this experiment were synthesized in an arc furnace utilizing a two-step process similar to that outlined in the work of Badica et al. [2]. An initial binary sample of BPt_3 was grown using Pt of purity 99.99 % and B of purity 99.999 %. In the final step of the sample growth, an excess amount of Li was added in order to account for losses during arc melting, giving a Li to BPt_3 ratio of 2.2:1. The crystal structure was verified via powder X-ray diffraction measurements. No impurity or binary phases were detected.

Prior to the magnetic relaxation measurements, the Li_2Pt_3B sample was characterized by means of measurements of electrical resistivity ρ, magnetization M, and specific heat C. All three measurements yielded a value of the superconducting critical temperature $T_c = 3.0$ K. This value is significantly higher than the values reported in the literature, the highest of which being $T_c = 2.4$ K [2]. Evidently, the value of T_c is rather sensitive to the composition of the sample, which could be a further indication that Cooper pairing is, indeed, unconventional in this compound.

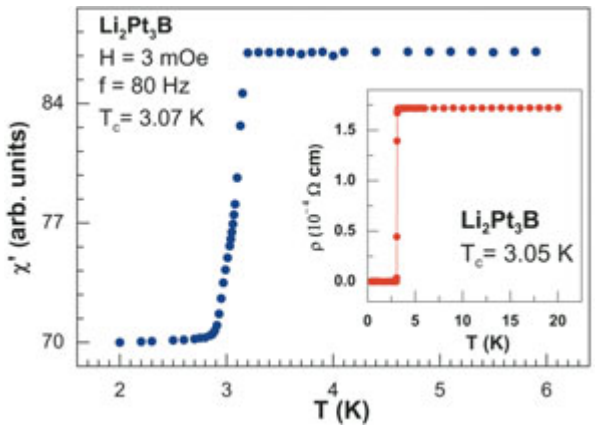

Fig. 1: Real part of the ac magnetic susceptibility, χ', as a function of temperature across the superconducting phase transition. Inset: electrical resistivity, ρ, as function of temperature.

The temperature dependence of the specific heat was measured using a quasi-adiabatic heat pulse method in a ^{3}He cryostat in the temperature range $0.6\ \mathrm{K} \le T \le 20\ \mathrm{K}$ and in magnetic fields up to $H \approx 4$ T. The specific heat in the normal state could be described by the expression $C(T) = C_e(T) + C_l(T)$, where $C_e(T)=\gamma T$ is the electronic contribution and $C_l(T) = \beta T^3$ is the lattice term. The best fit to the data yields $\gamma = 7.0$ mJ/(mol K^2) for the electronic specific heat coefficient and $\Theta_D = 203$ K for the Debye temperature, in good agreement with the values $\gamma = 7.0$ mJ/(mol K^2) and $\Theta_D = 228$ K reported by Takeya et al. [12]. A relatively sharp jump in the specific heat, $\Delta C = 15$ mJ/(mol K), was observed at the transition into the superconducting state, yielding a ratio $\Delta C / (\gamma T_c) = 1.2$, larger than the 0.8 value reported by Takeya et al. [12] but smaller than the weak coupling BCS value of 1.43. Below T_c, $C_e(T) \sim T^2$, consistent with the behavior reported previously [12] and in contrast to the exponential T-dependence expected for a BCS superconductor. The upper critical field, $H_{c2}(T)$, determined from the $C(T)$ measurements, increases linearly with decreasing temperature from T_c to $T = 0.6$ K and extrapolates linearly to a value of $H_{c2}(0) \approx 1.5$ T at $T = 0$ K.

We also characterized the superconducting transition of the sample by means of ac magnetic susceptibility measurements in a low ac field of $H = 3$ mOe and at a frequency of $f = 80$ Hz. This measurement was done with the sample situated inside a custom-built mixing chamber of a dilution refrigerator, using an inductance bridge with a SQUID as a null detector [13]. The midpoint of the superconducting transition for this sample is at $T_c = 3.07$ K and the transition width $\Delta T_c = 240$ mK. The data are displayed in Fig.1. In the inset of Fig. 1, we show the low temperature part of the electrical resistivity, $\rho(T)$, measured using a standard four-wires arrangement in a ^{3}He cryostat. $\rho(T)$ displays a sharp phase transition into the superconducting state with a transition width of $\Delta T_c = 55$ mK. $\rho(T)$ reaches zero at $T = 3.05$ K, in very good agreement with the susceptibility data. In the normal state, the $\rho(T)$ measurement revealed typical metallic behavior.

The investigation of vortex dynamics was performed in the 0.1 K – 2.8 K temperature range. Isothermal relaxation curves of the remanent magnetization M_{rem} were taken after cycling the specimen in an external dc magnetic field H. Vortices were introduced into the sample at a slow rate in order to avoid eddy current heating. After waiting for several minutes, the magnetic field was reduced to zero and the relaxation of the metastable magnetization recorded with a digital flux counter for several hours. The sample was prepared in the form of a thin slice, and the magnetic field was applied along the longest direction. At the lowest temperature of our investigation, $T = 0.1$ K, we determined the field corresponding to the Bean critical state, H_s, as the field where the remanent magnetization saturates as function of the external magnetic field. For this sample, we find $H_s = 200$ Oe at $T = 0.1$ K (cf. inset of Fig. 2). At higher temperatures the sample will be in the critical state

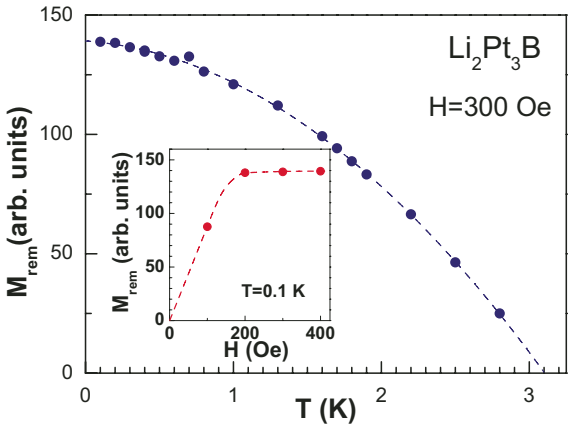

Fig. 2: Temperature dependence of the remanent magnetization M_{rem}. The dotted line is a parabolic fit to the data. Inset: M_{rem} as function of the external magnetic field at constant temperature, T=0.1 K. The dotted line is a guide to the eye.

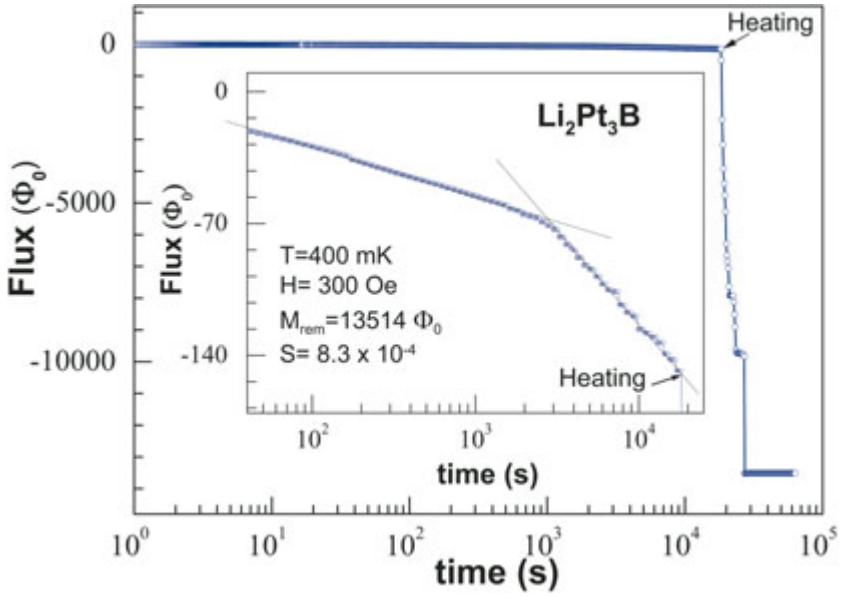

Fig. 3: A typical relaxation curve exemplified for T = 400 mK. The magnetic flux is measured as it is expelled out of the sample at constant temperature. After a certain time (marked by arrows in the figure), the sample is gradually heated and driven into the normal state. Inset: Two relaxation regimes are visible on an expanded scale.

already for smaller external fields as H_s decreases upon increasing T. In the main part of Fig. 2, we show values of the remanent magnetization obtained after cycling the sample in a field of H = 300 Oe as a function of temperature. M_{rem} decreases monotonically upon increasing the temperature with the experimental data well fitted by a parabola (dashed line in Fig. 2) which reaches zero at around $T \approx 3.1$ K. This is in excellent agreement with the value of T_c yielded by specific heat, ac susceptibility and electrical resistivity measurements.

A typical decay of the remanent magnetization from the critical Bean state at $T = 400$ mK is shown in Fig. 3. In this case, the creep was recorded for about 18000 s. At this time, the sample was heated above T_c in order to obtain the total value of the remanent magnetization as a sum of the amount decayed in the first 18000 s plus the quantity expelled on crossing T_c. This value is then used to normalize the creep rate. In the inset, the same data are displayed on an expanded scale. We can clearly distinguish two different logarithmic creep regimes. For 50 s < t < 2400 s, we observe a clear logarithmic relaxation law with an extremely low relaxation rate, $S = \partial \ln M / \partial \ln t = 8.3 \times 10^{-4}$. At around t = 2400 s, a sudden, strong increase of the relaxation rate occurs, following also a logarithmic law, but with a rate about a factor of four larger, $S = 3.1 \times 10^{-3}$. Indeed, an avalanche-like escape of vortices occurs around t = 2400 s, indicating a rather complex relaxation process. Vortices escaping the sample apparently need a considerable amount of time to overcome a certain barrier. We observed this type of regime change at all temperatures (see Fig. 4), except for relaxations below $T = 400$ mK and above $T = 2$ K. To our knowledge, this phenomenon of avalanches in the slow decay of vortices toward equilibrium has never been observed before in any superconductor, conventional or unconventional. This unexpected result points to new vortex physics in this noncentrosymmetric superconductor. The normalized temperature dependence of the relaxation rate, corresponding to the creep before the avalanches occur, is depicted in Fig. 5. In the upper panel, the rates are given in a double- logarithmic plot while, on the lower one, on linear scales. These rates are lower by a factor of five even than the very weak creep rates observed in $PrOs_4Sb_{12}$ [14], a superconductor that violates time reversal symmetry. As discussed by Sigrist and Agterberg [15], the lack of time reversal symmetry in such superconductors allows for the formation of flux-flow barriers formed by fractional vortices on domain walls of the superconductor that can prevent the motion of normal vortices. It is important to remark that almost the same anomalously weak creep rates as

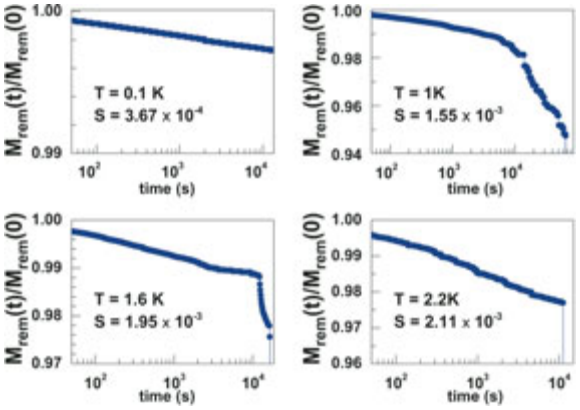

Fig. 4: Sequence of isothermal relaxation curves. Two relaxations regimes can be observed at intermediate temperatures as explained in the text.

in Li_2Pt_3Si have been observed for another non-centrosymmetric superconductor, $CePt_3Si$ [16]. The investigated $CePt_3Si$ sample was a high-quality single crystal which showed 13 % twinning in single-crystal X-ray diffraction.

We can speculate that the extremely slow motion of flux lines in Li_2Pt_3B could be caused by a new mechanism as recently proposed by Iniotakis et al. [17]. In many cases for non-centrosymmetric materials, the absence of an inversion center allows for the twinning of the crystal. These authors have shown theoretically, that a phase which violates time reversal symmetry can also be realized at interfaces separating crystalline twin domains of opposite spin-orbit coupling. In this case, flux lines with fractional flux quanta could exist on such interfaces and turn twin boundaries into strong barriers impeding flux creep. Within this model, vortex avalanches could be expected when such a fence opens due to excessive pressure of normal vortices. This is possible, if the vortex density increases to a level such that fractional vortices can no longer exist and the vortex pinning mechanism of twin boundaries fails. In the frame of this scenario, we can interpret the temperature window in which the avalanche effect has been observed in the following way. At temperatures below $T = 400$ mK, vortices move so slowly that the time necessary to build up the vortex density necessary to break a barrier, exceeds the observation time. For temperatures above $T = 2$ K, on the other hand, the overall density of vortices is strongly reduced (see Fig. 2), so that it becomes more difficult to reach the density required for demolishing barriers.

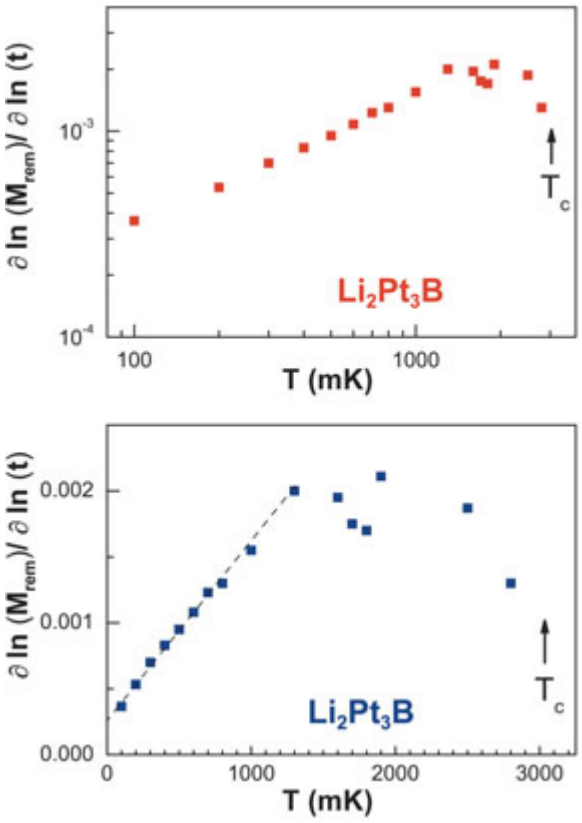

Fig. 5: The temperature dependence of the initial decay rate $S = \partial \ln M / \partial \ln t$ in a double logarithmic (upper panel) and a linear plot (lower panel).

However, one cannot rule out other scenarios which would account for the anomalous behavior discovered in this non-centrosymmetric superconductor, namely the strongest pinning ever observed followed by sudden avalanches.

In conclusion, we have observed in Li_2Pt_3B strong avalanches in the relaxation of the remanent magnetization. Prior to the avalanches, vortices move toward equilibrium for several hours with an extraordinarily slow creep rate, indicating that a new type of pinning is effective in this non-centrosymmetric superconductor. This type of pinning is different from the conventional pinning by defects, since it is effective only at low vortex densities. If the density of vortices leaving the sample increases close to the barrier which keeps them from moving, an avalanche occurs followed by creep rates that are about 5 to 10 times faster. This type of creep behavior has never been observed before.

References

[1] *K. Togano, P. Badica, Y. Nakamori, S. Orimo, H. Takeya, and K. Hirata,* Phys. Rev. Lett. **93** (2004) 247004.

[2] *P. Badica, T. Kondo, and K. Togano,* J. Phys. Soc. Jpn. **74** (2005) 1014.

[3] *U. Eibenstein and W. Jung,* J. Solid State Chem. **133** (1997) 21.

[4] *L .P.Gor'kov and E. Rashba,* Phys. Rev. Lett. **87** (2001) 037004.

[5] *P. A. Frigeri, D. F. Agterberg, A. Koga, and M. Sigrist,* Phys. Rev. Lett. **92** (2004) 097001.

[6] *V. M. Edelstein,* Phys. Rev. B **72** (2005) 172501.

[7] *E. Bauer, G. Hilscher, H. Michor, Ch. Paul, E.W. Scheidt, A. Gribanov, Yu. Seropegin, H. No□el, M. Sigrist, and P. Rogl, Phys. Rev. Lett.* ***92****, 027003 (2004).*

[8] *N. Kimura, K. Ito, K. Saitoh, Y. Umeda, H. Aoki, and T. Terashima,* Phys. Rev. Lett. **95** (2005) 247004.

[9] *T Akazawa, H. Hidaka, T. Fujiwara, T.C. Kobayashi, E. Yamamoto, Y. Haga, R. Settai, and Y. Ōnuki,* J. Phys. Cond. Matt. **16** (2004) L29.

[10] *H. Q. Yuan, D. F. Agterberg, N. Hayashi, P. Badica, D. Vandervelde, K. Togano, M. Sigrist, and M. B. Salamon, Phys.* Rev. Lett. **97** (2006) 017006.

[11] *M. Nishiyama, Y. Inada, and Guo-qing Zheng,* Phys. Rev. Lett. **98** (2007) 047002.

[12] *H. Takeya, E. ElMassalami, S. Kasahara, and K. Hirata,* Phys. Rev. B **76** (2007) 104506.

[13] *A. Amman, A. C. Mota, M. B. Mapl,e and H. v. Löhneysen,* Phys. Rev. B **57** (1998) 3640.

[14] *T. Cichorek et al, to be published.*

[15] *M. Sigrist and D. Agterberg,* Prog. Theor. Phys. **102** (1999) 965.

[16] *C.F. Miclea, A.C. Mota, M. Nicklas, M. Sigrist, R. Cardoso, F. Steglich, and E. Bauer, in preparation.*

[17] *C. Iniotakis, S. Fujimoto, and M. Sigrist,* J. Phys. Soc. Jpn. **77** (2008) 083701.

---

[1] Max-Planck Institute for Chemical Physics of Solids, Dresden, Germany

[2] Department of Physics and Institute for Pure and Applied Physical Sciences, University of California, San Diego, La Jolla, California, USA

[3] Solid State Laboratory, ETH-Zurich, Zurich, Switzerland

[4] Institute for Theoretical Physics, ETH-Zurich, Zurich, Switzerland